RESEARCH   **Open Access**

The role of diffusion-weighted MRI in assessment of response to chemotherapy in osteosarcoma

Tarek Ahmed Raafat[1*] ⓘ, Randa Osama Kaddah[2], Lobna Mohamed Bokhary[2], Hend Ali Sayed[2] and Ahmed Sayed Awad[3]

Abstract

Background: The most effective treatment for osteosarcoma is neoadjuvant chemotherapy along with surgical resection of the tumor. The prognosis significantly correlates with the degree of tumor necrosis following preoperative chemotherapy. The tumor necrosis will result in loss of the cell membrane integrity and expansion of the extracellular diffusion space which can be detected as an increase in the mean ADC value. The aim of our work is to evaluate the use of diffusion-weighted imaging (DWI) and apparent diffusion coefficient (ADC) value measurement for monitoring the therapeutic response after chemotherapy in osteosarcoma.

Results: This study included 25 cases of osteosarcoma: 15 males and 10 females. The age of the patients ranged from 7 to 46 years with mean age 22 years. All were assessed by magnetic resonance imaging (MRI) including DWI and the mean and minimum ADC values were calculated before and after chemotherapy. Follow-up DWI post-therapy revealed a rise in mean ADC value in 17 patients who considered having good response. The ADC value had been raised from $1.05 \pm 0.4 \times 10^{-3}$ mm^2/s to $1.82 \pm 0.45 \times 10^{-3}$ mm^2/s (P < 0.027) that is statistically moderately significant. In 8 patients, the post-therapy ADC value was similar to that of pre- or with a little change and they were considered having poor response. It showed changes from $1.29 \pm 0.35 \times 10^{-3}$ mm^2/s to $1.32 \pm 0.36 \times 10^{-3}$ mm^2/s (P > 0.05) that means no significant difference.

Conclusion: DWI and ADC value measurement play an important role in monitoring the therapeutic response after chemotherapy in osteosarcoma patients by comparing the mean ADC values before and after treatment.

Keywords: Diffusion MRI, Response to chemotherapy, Osteosarcoma

Background

Osteosarcoma is the most common bone sarcoma in children and adolescents [1]. The combination of pre- and postoperative chemotherapy with surgery significantly increased the survival rate for osteosarcoma patients [2].

The prognosis significantly correlates with the degree of tumor necrosis following preoperative chemotherapy [3]. If the treatment response could be assessed before

surgery by non-invasive method, this may help avoid in-effective chemotherapy and invasive biopsies as well as determine surgical timing [4].

Traditionally, the tumor response to chemotherapy was assessed by comparison of changes in tumor size by images obtained before and after therapy. For osteosarcoma, there is a specific problem: during successful chemotherapy, tumor size does not diminish significantly because the therapy has only limited impact on the mineralized matrix of the tumor [5, 6].

Magnetic resonance imaging (MRI) and fluorine-18 fluorodeoxyglucose combined positron emission tomography/computed tomography (18F FDG PET/CT) have

* Correspondence: tarek2005_8@yahoo.com
[1]Radiology Department, National Cancer Institute, Cairo University, Giza, Egypt
Full list of author information is available at the end of the article

been used to assess osteosarcoma during neoadjuvant chemotherapy. 18F FDG PET/CT calculates the metabolic activity by using maximum standardized uptake value (SUVmax) [7]. Change of SUV after neoadjuvant chemotherapy is useful in predicting treatment response [8]. However, the delineation of tumor margins on 18F FDG PET/CT is difficult, and monitoring responses is problematic when the uptake is increased by inflammation or reactive fibrosis [7].

Also in standard MRI study, it still has limited ability for proper assessment of treatment responses as sometimes treated lesions show residual contrast enhancement and often increase in size despite pathological response [4].

DWI is a non-contrast functional MR imaging technique. It helps in the analysis of tissue characteristics based on the diffusion of water protons within the tissue. Quantitative assessment of a mass is possible by calculating its apparent diffusion coefficient (ADC) value which is inversely correlated with tissue cellularity. Treatment with chemotherapy can result in tumor necrosis, loss of the cell membrane integrity, and expansion of the extracellular diffusion space which can be detected as an increase in the mean ADC value for the tumor [9].

The primary objective of our study was to evaluate the potential of DWI and calculated ADC value (as part of functional imaging) for monitoring the therapeutic response to chemotherapy in osteosarcoma and to compare the ADC values before and after chemotherapy.

Methods

The Institutional Review Board of our Radiology Department approved the design of the study and the use of clinical data. Written consent was obtained from the patients or their parents prior to the procedures.

This study included 25 patients (10 females and 15 males), their ages range from 7 to 46 years with mean age 22 years. They were referred to radiology department from the surgical and clinical oncology departments.

The flow chart of our study is illustrated in Fig. 1.

Inclusion criteria

Patients who are primary diagnosed to have osteosarcoma, candidates or already had MR imaging and will follow the neoadjuvant chemotherapy regimens.

All patients are histologically proven to be osteosarcoma patients.

Exclusion criteria

Patients with other concurrent systematic diseases that would harm the safety of the patient or the patient's ability to complete the study were excluded.

General criteria of contra-indication to MRI are as follows: patients with pace maker, cochlear implants, cerebral aneurysm clips, and ocular metallic foreign body.

All patients were subjected to the following:

1. Clinical assessment and history taking.
2. Laboratory investigations including renal function tests and bleeding profile tests.
3. Revision of previous radiological investigations and histopathological reports.
4. Two MR examinations were performed as follow: the first before the neoadjuvant chemotherapy, and the second after 3 to 6 months after the preoperative neoadjuvant chemotherapy.

MRI protocol

MRI was performed on high field system (1.5 Tesla) closed magnet unit (Phillips Achieva XR). A Sense –XL –torso (16 channels) phased array coil was used for chest and pelvis while surface coil was used for lesions of the extremities. A combination of axial, sagittal, and coronal images was obtained using T1-weighted spin-echo sequence (TR "average", 500 ms; TE, 10–15 ms), T2-weighted fast spin-echo sequence (TR, 4000–5000 ms; TE, 110–120 ms; TF, 17–25) and short time inversion recovery "STIR" sequence (TR "average", 5000 ms; TE, 25 ms; TI, 160 ms; TF, 17). These sequences were obtained with 5-mm slice thickness, 1-mm interslice gap, and 256×196 matrix size.

DWI was performed in the axial plane with parallel image and sensitivity phase encoding (SENSE) with the following parameters: TR, 4000–5000 ms; TE, 110–120 ms; 220 mm FOV; 128×64 pixel matrix size; 5-mm slice thickness; and 1-mm interslice gap. DWI was acquired with diffusion gradient encoding in 3 orthogonal directions with b values (0/50/400/800 s/mm2). In all images, a fat-saturated pulse was used to exclude chemical-shift artifacts. ADC map images and quantitative DWI analysis (ADC measurement) were done.

Contrast-enhanced images of axial, sagittal, and coronal plane were obtained using a T1-weighted spin-echo sequence with and without fat suppression (TR, 450–650 ms; TE, 10–16 m; matrix size, 256×256; slice thickness, 5 mm; 1-mm interslice gap) after the injection of 0.1 mmol/kg of body weight of gadopentetate dimeglumine injected at 2 ml/s, followed by a 20 ml normal saline flush.

THRIVE (T1-weighted high-resolution isotropic volume excitation, fast gradient, 3D and Fat-sat) was obtained with following parameters (TR, 4.5 ms; TE, 2.2 ms; matrix size, 300×300; FOV, 220 mm; slice thickness, 3.6 mm; 3D thickness 3, 0-mm interslice gap).
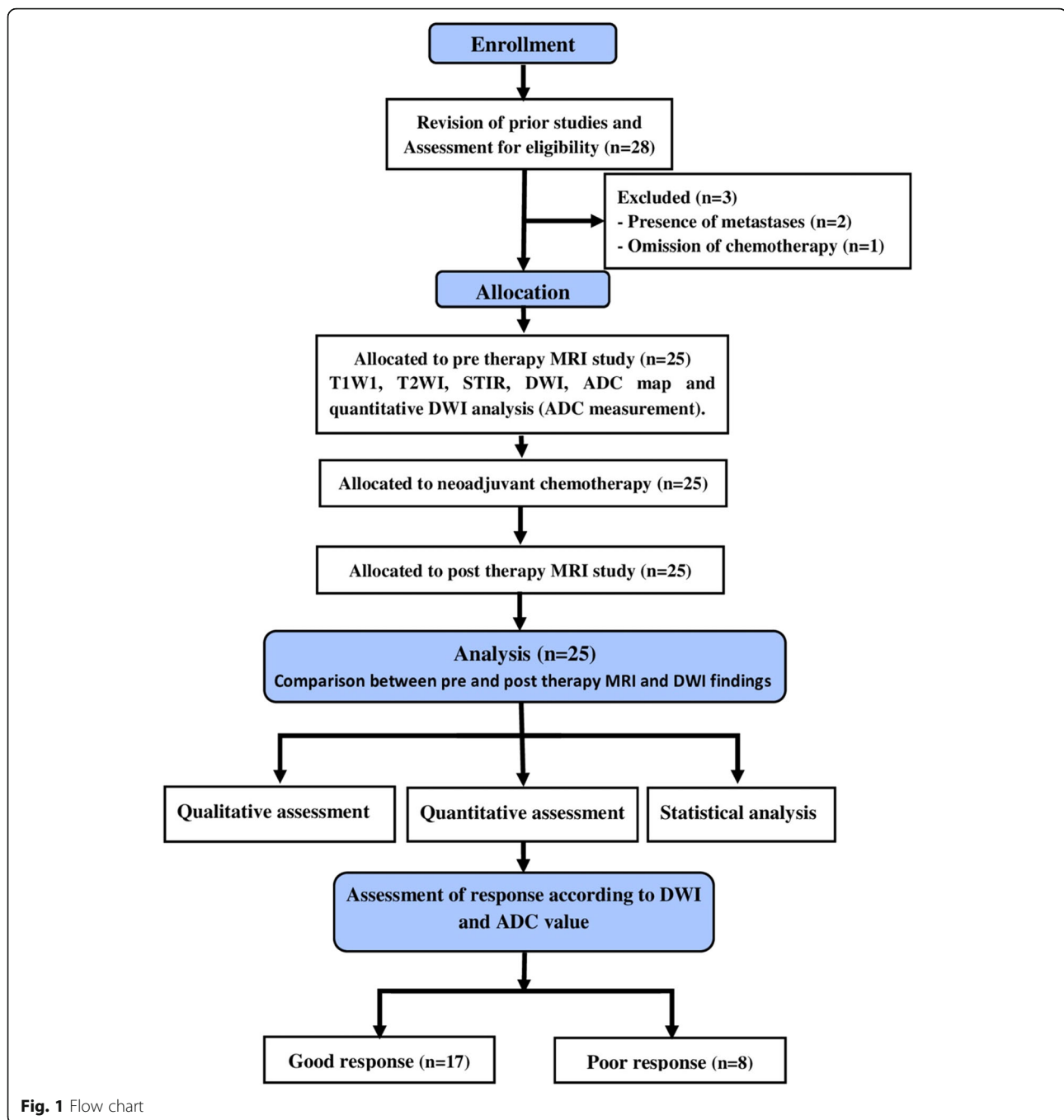
Fig. 1 Flow chart

Image analysis

All pre- and post-chemotherapy MRI studies were downloaded from DICOM server to workstation, and two radiologists experienced on musculoskeletal radiology analyzed the images. The assessment of the lesions was done first in the conventional MRI then in the DWI with ADC calculation.

Standard MRI analysis

In the initial pre-therapy MRI study, each lesion was identified on conventional MRI and the morphological features were recorded including site, size, signal characteristics, tumor breakdown, pattern, and intensity of contrast uptake. Assessment of the osteosarcoma behavior was reported including medullary involvement,

pattern of bony cortex affection (either subtle cortical breaching or frank cortical destruction), associated soft tissue component, and skip lesions. The extent of local infiltration in each lesion was assessed including muscle invasion, crossing of fascial boundaries, and neurovascular compromise.

DWI analysis
Qualitative analysis
This was done by studying the signal intensity of different lesions on DWIs (at the highest b-value, i.e., at 800 s/mm^2) and the ADC map. If all or part of the lesion is of high signal in DWI and low in ADC map, it is considered as diffusion restriction.

Quantitative analysis
Measurements of the ADC value were made using electronic cursor on the ADC map in different regions of interest (ROI) of the lesion. As the osteosarcoma shows inhomogeneous signal intensity, ADC measurements can highly change from a slice to another and from an area to another in the same slice. So we do the following to overcome these obstacles:

Place the ROI in solid and preferably enhancing parts of the lesion.

Avoid including areas that may influence the ADCs as necrotic, fibrotic, and hemorrhagic areas as well as adjacent fat, normal tissue, and bone. This was facilitated by using the pre- and post-contrast MR images, mainly the T2 and post-contrast THRIVE MR images as source images for the ROI placement.

We follow the methods of Lee SK et al. [4] and Lee SY et al. [10] in ADC measurement. We measure the mean ADC (obtained from the single-section ROI) that contained the largest part of the tumor. Also we measure minimum ADC (obtained from the single-section ROI) but placing ROI in the lowest signal intensity within the solid part of the tumor on the ADC map that presented as a hyperintense SI on DWI. To select the lowest ADC value, small ROI (minimum area, 0.5 cm^2) were drawn 3–5 times and the minimum was recorded.

Also, in patients complicated with pathological fractures. This could affect the ADC measurements. However in our study, we avoid placement of ROI in and adjacent to site of fracture to reduce as much as possible error in ADC value.

Follow-up MRI
Follow-up MRI examinations of average 3–6 months after chemotherapy administration were done. The lesions were evaluated in the same way of the pre-therapy MRI. The changes that occurred between the imaging dates before the start of initial treatment and the most recent follow-up examination were evaluated and documented to assess the response to treatment.

In addition, the ADC ratio was calculated by using the following formula to evaluate the relative change in the pre- and post-chemotherapy ADC values of osteosarcomas: $ADC_{ratio} = (ADC_{post} - ADC_{pre})/ADC_{pre}$.

To assess the tumor response to chemotherapy, we depend upon the rule of the ADC value is inversely correlated with tissue cellularity of the lesion. Treatment with chemotherapy can result in loss of the cell membrane integrity which can be detected as an increase in the mean ADC value for the tumor [9]. So, the response to treatment was classified in good response and poor response according to degree increase in ADC value and ADC_{ratio}. Also, we evaluate the changes in tumor size, breakdown, and pattern of enhancement.

Statistical analysis
Statistical analysis was performed using the statistical software: SPSS statistical package version 21 (SPSS Inc., Chicago, IL).

Numerical data were expressed as mean and standard deviation or median and range as appropriate. Qualitative data were expressed as frequency and percentage.

MRI features that were analyzed included the location, size, shape, and margins of the lesion, signal characteristics, enhancement patterns, pattern of diffusion, and ADC value.

Results
The study population included 25 patients, 10 females and 15 males, all were histopathologically diagnosed as osteosarcoma. The age of the patients ranged from 7 to 46 years with mean age 22 years, 64% of the patients were ≤ 20 years.

The study included 22 cases involving the long bones of the extremities, 3 cases (13.6%) involving the upper limb long bones and 19 cases involving the lower limb long bones (86.3%). 47.4% of the lower limb cases involved the epi-meta-diaphyseal region, while 36.3% involved the meta-diaphyseal region, 21.1% involved the surface of the bone, and 5.3% involved the short bones. Osteosarcoma in upper limbs showed equal percent in epi-meta-diaphyseal, meta-diaphyseal, and epiphyseal regions. Three patients had osteosarcoma in the axial skeleton particularly in the iliac bones.

Most of osteosarcoma cases in our study (96%) elicit low signal in T1WI; 52% of total patients showed high signal in T2WI. After contrast administration, 92% of cases showed heterogeneous pattern of enhancement, 8% showing homogenous contrast uptake. Cystic breaking down was present in 72% of the patients and 60% of lesions presented with internal hemorrhagic areas.

Lesion size was assessed in contrast enhanced images and was ranging from 3.4 up to 22.9 cm with mean size of 9.4 cm.

All cases showed associated extra osseous soft tissue component. They showed medullary involvement in 22 cases (88%) with 6 cases (24%) showing subtle cortical breaching while 14 cases (56%) showed frank cortical bony destruction. Eleven cases (44%) showed articular extension and 13 cases (52%) had neurovascular involvement. Skip lesions were found in 5 cases (20%). Pathological fracture was found in 2 cases (8%).

The qualitative DWI was done showing bright signal in high b values of 100% of lesions when compared to the normal nearby muscles. Quantitative DWI and ADC mapping was done for all cases with detailed analysis of ADC values (Table 1).

Follow-up MRI assessment

On follow-up MRI after the neoadjuvant chemotherapy, comparison of the pre- and post-therapy images was done for each patient. The response to treatment was determined according to changes in tumor size, breakdown, pattern of enhancement, degree of diffusion restriction, and ADC value. The constellation of post-therapy MRI findings revealed 17 patients with good response, 8 patients with poor response.

As we could not confidently differentiate viable and necrotic tumor tissue on T2WI because both show similar T2 relaxation times, therefore, we used contrast-enhanced T1WI to evaluate the tumor viability in post-treatment images. In patients with good response, most of the tumor was not enhanced in 10 patients while in 7 patients, there was little enhancement with size reduction on the post-treatment images. In patients with poor response, in 4 patients, there was residual intense enhanced tumor without interval decrease in size on a post-treatment images. While in 4 patients, most of the tumor was enhanced, despite interval decrease in extent of enhanced area.

Follow-up DWI post-therapy revealed a rise in mean ADC value in 17 patients who considered having good response (Figs. 2, 3, and 4). The ADC value had been raised from $1.05 \pm 0.4 \times 10^{-3}$ mm^2/s to $1.82 \pm 0.45 \times 10^{-3}$ mm^2/s ($P < 0.027$) that is statistically moderately significant (Table 2).

In 8 patients, the post-therapy ADC value was similar to that of pre- or with a little change and they were considered having poor response (Fig. 5). It showed changes from $1.29 \pm 0.35 \times 10^{-3}$ mm^2/s to $1.32 \pm 0.36 \times 10^{-3}$ mm^2/s ($P > 0.05$) that means no significant difference (Table 3).

The post-neoadjuvant chemotherapy ADC value in patients with good response was higher than that of poor response ($P < 0.01$).

The patients with a good response had a significantly higher ADC ratio than those with a poor response (0.73 ± 0.22 and 0.06 ± 0.29 respectively).

Follow-up MR showed increased intra-tumoral breaking down in 13 patients (52%). Comparison between breaking down noted in the initial MRI and after treatment was statistically significant (P value = 0.0008). Post-neoadjuvant chemotherapy necrotic tumor areas showed mean ADC value was $2.43 \pm 0.25 \times 10^{-3}$ mm^2/s. Viable tumor areas revealed lower ADC value (mean $1.04 \pm 0.25 \times 10^{-3}$ mm^2/s). The difference in ADC between viable and necrotic tumor areas was highly significant ($P < 0.01$).

Discussion

Monitoring the chemotherapy effect for osteosarcoma patients is mandatory in order to plane for surgical procedures and postoperative chemotherapy. Recently the gold standard for judging the curative effect of chemotherapy is detecting tumor necrosis rate using histological method, but this method is traumatic due to repeated biopsy [6].

DWI is a non-invasive imaging method for measuring the local diffusion characteristics of water molecules in vivo. It can give information about spatial composition and the functional status of water exchange among various tissues in pathophysiological states from the molecular level. Accordingly, it can detect the early morphological and pathological changes of related to water content of tissue and ADC value can reflect the degrees of tissue water diffusion [11].

Predicting the response to chemotherapy in osteosarcoma cases can be well assessed by increasing ADC from baseline when the tumor which shows good response to therapy. Its use in the follow-up of treated tumors

Table 1 Detailed analysis of ADC values

	Minimum ADC (× 10^{-3} mm^2/s)	Mean ADC (× 10^{-3} mm^2/s)
Mean	0.81	1.13
Median	0.68	1.07
Minimum	0.13	0.54
Maximum	1.90	2.1

The mean ADC value was ≤ 1.3 × 10^{-3} mm^2/s in 76% of cases
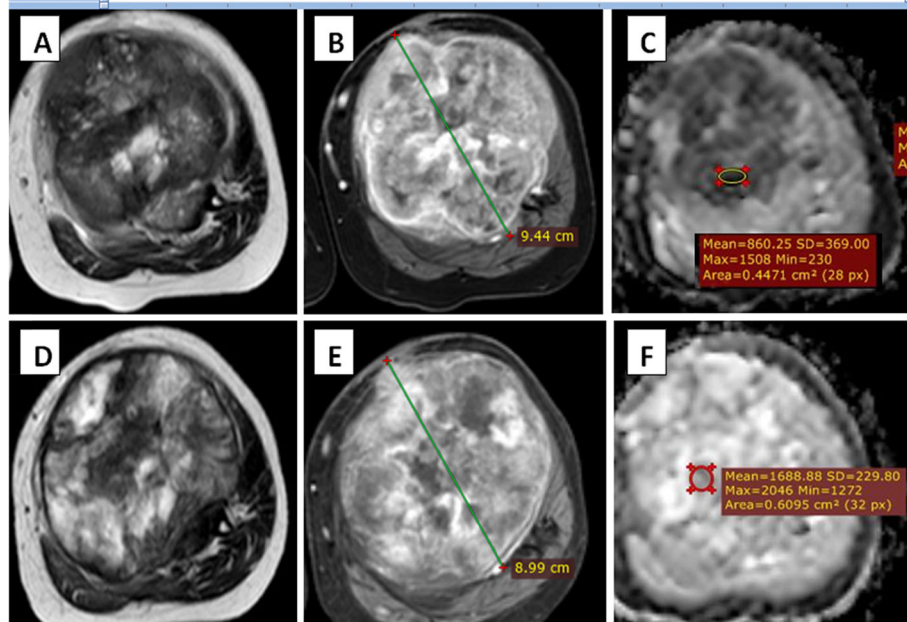
Fig. 2 A 22-year-old male with osteosarcoma in the left proximal tibia. MR images **a**–**c** before and **d**–**f** after chemotherapy. **a**, **b** Axial T2-WI and contrast-enhanced T1-WI showing left upper tibial intra medullary infiltrative lesion associated with extra osseous soft tissue component. It elicits high T2 signal and heterogeneous post contrast enhancement with areas of necrosis and cystic degeneration. **c** ADC map revealed patchy diffusion restriction of the lesion with mean ADC value (mean, 0.86×10^{-3} mm^2/s). **d**, **e** Follow-up axial T2-WI and contrast-enhanced T1-WI showing slight size regression with less contrast uptake. **f** Follow-up ADC map showing elevated ADC values (mean, 1.68×10^{-3} mm^2/s) denoting good therapeutic response
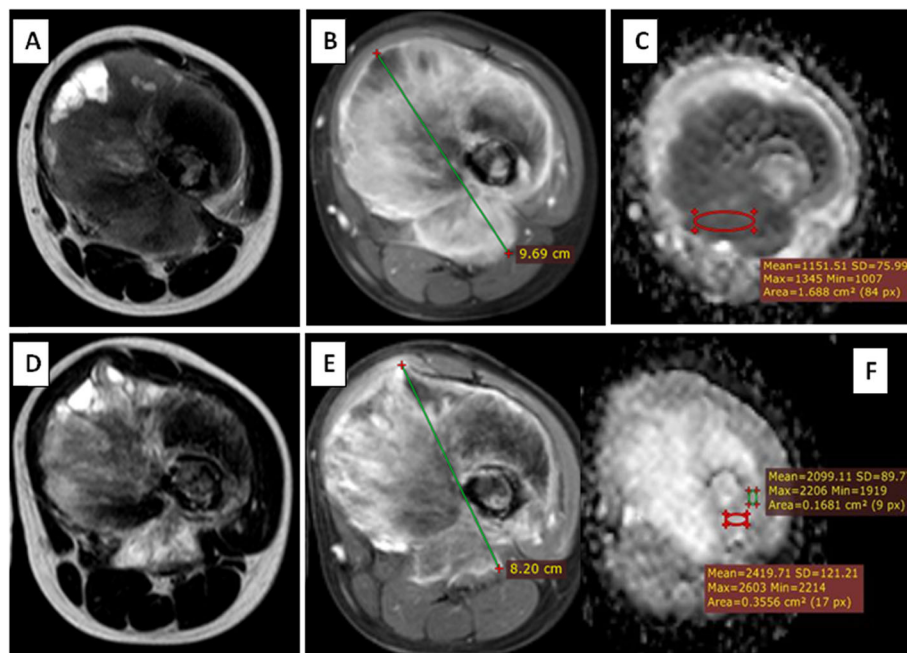
Fig. 3 A 7-year-old female with osteosarcoma in the left femur. MR images **a**–**c** before and **d**–**f** after chemotherapy. **a**, **b** Axial T2-WI and post contrast-enhanced T1-WI showing left femur intra medullary infiltrative lesion with circumferential soft tissue mass eliciting heterogeneous mixed signal in T2 and heterogeneous contrast uptake. **c** ADC map showed diffusion restriction with mean ADC values of the most restricted ROIs about (mean, 1.1×10^{-3} mm^2/s). **d**, **e** Follow-up axial T2-WI and contrast-enhanced T1-WI showing minimal size regression with heterogeneous enhancement. **f** Follow-up ADC map showing elevated ADC values (mean, 2.30×10^{-3} mm^2/s) denoting good therapeutic response
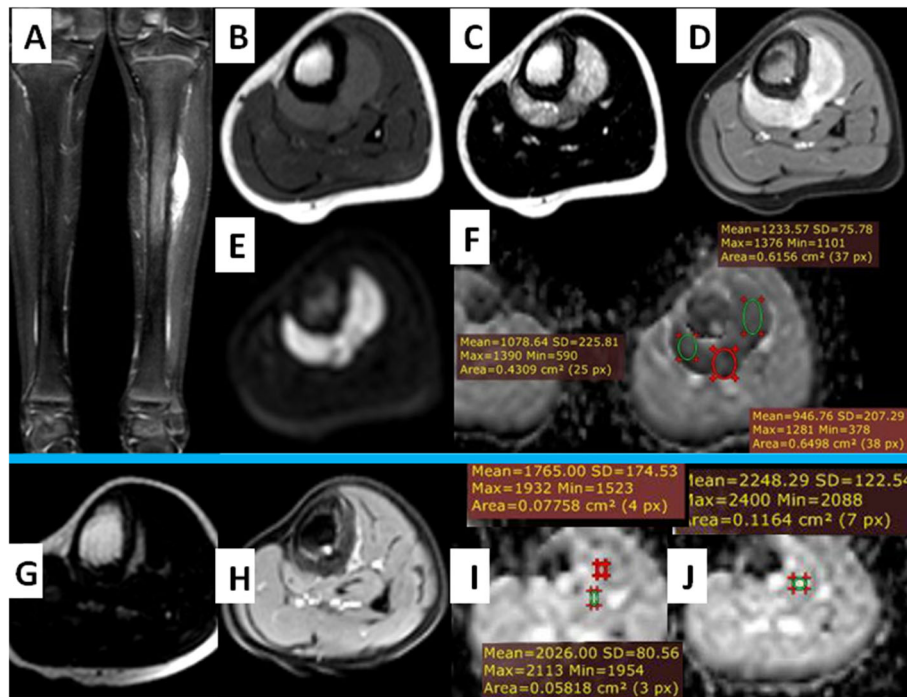
Fig. 4 A 9-year-old female, diagnosed as parosteal osteosarcoma of left tibia. MR images **a–f** before and **g–j** after chemotherapy. **a–d** Coronal STIR, Axial T1, T2-WI and contrast-enhanced T1-WI showing cortically based diaphyseal mass lesion circumferentially involving the anterolateral and posterior surfaces of the left tibial mid shaft with thickening of the cortex. It elicits heterogeneous high signal in STIR, low signal in T1, high signal in T2, with heterogeneous contrast uptake. **e, f** DWI and ADC map showed diffusion restriction with mean ADC values about (mean, 1.08×10^{-3} mm^2/s). **g, h** Follow-up axial T2 and axial post contrast showing marked regression in the size and enhancement of the mass. **i, j** Follow-up ADC mapping and ROI inserted over the most restricted areas revealed increase in the values (mean values of 2×10^{-3} mm^2/s) denoting good therapeutic response

appears assessed by comparing the post-chemotherapy value by the initial ADC value [12]

This study included 25 patients (15 males and 10 females); their ages ranged from 7 to 46 years old with mean 22.04, nearly matching the review done by Wang et al. [11], whom study included 30 patients of which their ages ranged from 7 to 65 years old with mean 26.8.

We found that there is a slight male predilection in our study (male 60% and female 40%), matching Uhl et al. [6] study, while contrasting Oka et al. [13] study which showed female predilection.

In our study, the most common site for osteosarcoma was around knee with predilection of distal femur matching Tirman et al. [14] study but with higher percent, in which knee site was accounting for about (35%) in the latter study, while it accounts for about (56%) in our study. The metaphysis of long bones were the most commonly affected site in our study matching the same

study with percent 78.2% in our study comparing to 80% in Triman et al. [14] study. In our study, there was extension to the epiphysis in 47.8% which is slightly lower than Triman et al. [14] study which was 57%.

Flat bones affection was of very low percent in our study 8% matching Triman et al. [14] and Ottaviani et al. [15] studies but with lower percent, in which it was 20% in the former study.

According to the literature and previous studies, most of the lesions exhibit low T1WI (lower than muscle) and high T2WI (similar to that of fat or fluid) signal intensities [16]. High signal intensity in T2WI in our study represented 52% of all cases matching Greenspan et al. [16] study. There was no significant difference on T2WI between viable and necrotic tumor tissue because the T2 relaxation times were similar making the assessment of tumor viability based on T2WI difficult. This matches with study of Uhl et al. [6].

Table 2 Analysis of mean ADC values in good response cases

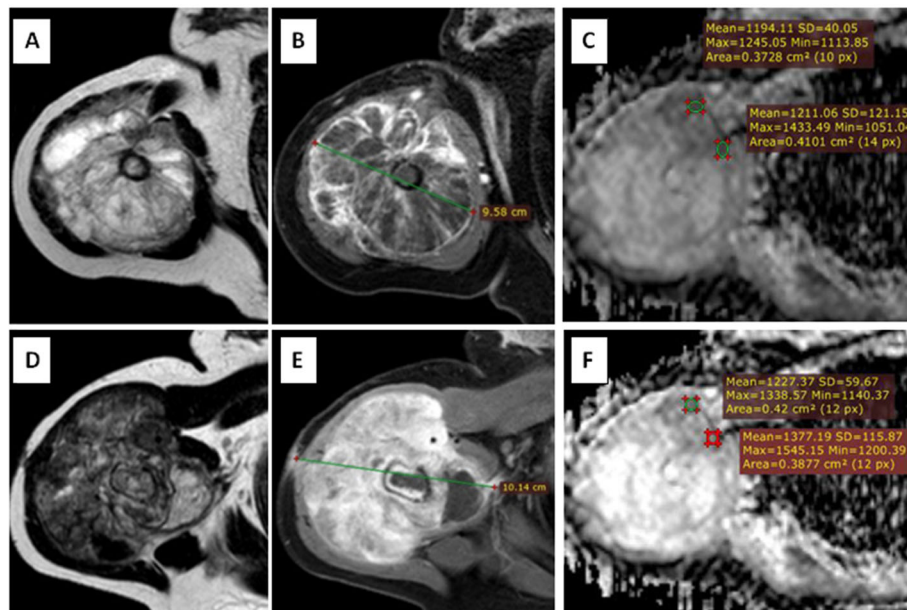| DWI (mean ADC value) $\times 10^{-3}$ mm^2/s	Mean	No. of patients	Std. deviation	Mean difference	P value
Initial MRI	1.0553	17	0.40884	− 0.7735	< 0.027
Follow-up MRI	1.8288	17	0.45761		

Fig. 5 A 18-year-old male with osteosarcoma in the right humerus. MR images **a**–**c** before and **d**–**f** after chemotherapy. **a**, **b** Axial T2-WI and contrast-enhanced T1-WI showing cortically based meta-diaphyseal mass lesion circumferentially surrounding the right humerus infiltrating its medulla all over the shaft. It elicits heterogeneous high signal in T2 with heterogeneous contrast uptake. **c** ADC map showed diffusion restriction with mean ADC values of the most restricted ROIs about (mean, 1.29×10^{-3} mm^2/s). **d**, **e** Follow-up conventional axial T2 and post contrast showing size progression and more contrast enhancement. **f** Follow-up ADC mapping showed no significant interval changes (1.3×10^{-3} mm^2/s) indicating poor response

We found intra-tumoral hemorrhagic component in 60% of all cases represented as high T1WI signal, while intra-tumoral cystic breakdown were found in 72% of cases.

Yakushiji et al. [17] found similarity of enhancement in 22 cases of different types of osteosarcoma; they found the lesions have either avid heterogeneous enhancement in 18 cases or peripheral rim with enhancement of the internal septae in 4 cases, nearly matching our results that the majority 18 cases showed avid heterogeneous and 7 cases showed peripheral rim enhancement with enhancement of the septae.

Qualitative DWI was done for our osteosarcoma cases pre- and post-treatment, showing homogenous and heterogeneous bright signals in high b-values. ADC mapping was done with measurement of mean ADC value. In our study, the average mean ADC for all the pre-chemotherapy cases was $1.13 \pm 0.40 \times 10^{-3}$ mm^2/s, and the average minimum ADC was $0.81 \pm 0.50 \times 10^{-3}$ mm^2/s.

Compared to many studies that worked on DWI and ADC mapping of osteosarcoma, Bajpai et al. [18] revealed average mean ADC in pre-chemotherapy cases equal to $1.29 \pm 0.22 \times 10^{-3}$ mm^2/s. Oka et al. [13] revealed average mean ADC $1.20 \pm 0.25 \times 10^{-3}$ mm^2/s while average minimum ADC was $0.88 \pm 0.16 \times 10^{-3}$ mm^2/s. Wang et al. [11] study revealed mean ADC value of pre-chemotherapeutic cases about $1.24 \pm 0.17 \times 10^{-3}$ mm^2/s. These values are nearly matching our study; however, Uhl et al. [6] found in their study that the mean ADC of untreated tumor was $2.1 \pm 0.4 \times 10^{-3}$ mm^2/s.

Generally, malignant bone tumors show lower ADC compared to benign bone tumors. However, it has been reported that certain types of benign bone tumor may present low ADC ($< 1.0 \times 10 - 3$ mm2/s), such in the case of non-ossifying fibroma or giant cell tumor. Thus, DWI should not be used alone, but in addition to conventional MRI sequences [19].

The response to treatment was determined according to changes in tumor size, breakdown, pattern of

Table 3 Analysis of mean ADC values in poor response cases

DWI (mean ADC value) $\times 10^{-3}$ mm^2/s	Mean	No. of patients	Std. deviation	Mean difference	P value
Initial MRI	1.2529	8	0.35236	− 0.0685	> 0.05
Follow-up MRI	1.3214	8	0.36576		

enhancement, degree of diffusion restriction, and ADC calculation. It is very important to assess the tumor breaking down post-neoadjuvant treatment by conventional MRI, in which we found that there was increased in tumor breaking down in post-therapeutic conventional MR follow-up imaging with statistically significant P value (P value = 0.0008) when compared to the initial MRI.

In our study, the constellation of post-therapy standard MRI and DWI findings revealed 17 patients with good response and 8 patients with poor response.

Many studies [6, 11, 13] assessed the role of DWI and ADC value in follow treatment of osteosarcoma. Those studies revealed increase in the mean ADC value after treatment. Uhl et al. [6] found that post-treatment mean ADC value has been raised to $2.5 \pm 0.4 \times 10^{-3}$ mm^2/s. Wang et al. [11] found that post-treatment mean ADC value has been raised to $1.93 \pm 0.39 \times 10^{-3}$ mm^2/s. Oka et al. [13] found that post-treatment mean ADC value has been raised to $1.80 \pm 0.44 \times 10^{-3}$ mm^2/s.

This matches our study that showed a rise in average mean ADC value of the 17 patients with good response being raised from $1.05 \pm 0.4 \times 10^{-3}$ mm^2/s to $1.82 \pm 0.45 \times 10^{-3}$ mm^2/s with P value < 0.027.

So the DWI and ADC value in addition to standard MRI findings can distinguish viable and necrotic tumor areas and then noninvasively, dynamically, early detect curative effect of chemotherapy in malignant tumor.

The limitations of our study included the relatively small number of cases and lack of correlation with post-chemotherapy pathological results or sizeable comparative group using another functional imaging modality as 18F-FDG-PET/CT.

Conclusion

The combination of pre- and postoperative chemotherapy with surgery significantly increased the survival rate for osteosarcoma patients. The prognosis significantly correlates with the degree of tumor necrosis following preoperative chemotherapy. DWI and measuring ADC values play an important role in monitoring this therapeutic response by comparing the mean ADC values pre- and post-treatment. So, it adds more diagnostic specificity, confirms the utility of DWI as a biomarker, and also may be considered as virtual biopsy in such conditions.

Abbreviations

OS: Osteosarcoma; MRI: Magnetic resonance imaging; DWI: Diffusion-weighted imaging; ADC: Apparent diffusion coefficient; 18F FDG PET/CT: Fluorine-18 fluorodeoxyglucose combined positron emission tomography/computed tomography; SUVmax: Maximum standardized uptake value; ROI: Region of interest; THRIVE: T1-weighted high-resolution isotropic volume excitation

Author details

[1]Radiology Department, National Cancer Institute, Cairo University, Giza, Egypt. [2]Radiology Department, Faculty of Medicine, Cairo University, Giza, Egypt. [3]Diagnostic and Interventional Radiology, Faculty of Medicine, Cairo University, Giza, Egypt.

References

1. Flores RJ, Kelly AJ, Li Y, Nakka M, Barkauskas DA, Krailo M, Man TK (2017) A novel prognostic model for osteosarcoma using circulating CXCL10 and FLT3LG. Cancer 123(1):144–154. https://doi.org/10.1002/cncr.30272
2. Kubo T, Furuta T, Johan MP, Ochi M, Adachi N (2017) Value of diffusion-weighted imaging for evaluating chemotherapy response in osteosarcoma: a meta-analysis. Mol Clin Oncol 7(1):88–92. https://doi.org/10.3892/mco.2017.1273
3. Huang B, Wang J, Sun M et al (2020) Feasibility of multi-parametric magnetic resonance imaging combined with machine learning in the assessment of necrosis of osteosarcoma after neoadjuvant chemotherapy: a preliminary study. BMC Cancer 20:322. https://doi.org/10.1186/s12885-020-06825-1
4. Lee SK, Jee W-H, Jung CK, Im SA, Chung N-G, Chung Y-G (2020) Prediction of poor responders to neoadjuvant chemotherapy in patients with osteosarcoma: additive value of diffusion-weighted MRI including volumetric analysis to standard MRI at 3T. PLoS One 15(3):e0229983. https://doi.org/10.1371/journal.pone.0229983
5. Huang WY, Wen JB, Wu G, Yin B, Li JJ, Geng DY (2016) Diffusion-weighted imaging for predicting and monitoring primary central nervous system

lymphoma treatment response. AJNR 37(11):2010–2018. https://doi.org/10.3174/ajnr.A4867

6. Uhl M, Saueressig U, Koehler G, Kontny U, Niemeyer C, Reichardt W, Langer M (2006) Evaluation of tumour necrosis during chemotherapy with diffusion-weighted MR imaging: preliminary results in osteosarcomas. Pediatr Radiol 36(12):1306–1311

7. Byun BH, Kong CB, Lim I, Choi CW, Song WS, Cho WH et al (2013) Combination of 18F-FDG PET/CT and diffusion-weighted MR imaging as a predictor of histologic response to neoadjuvant chemotherapy: preliminary results in osteosarcoma. J Nucl Med 54(7):1053–1059Epub 2013/05/15 PMID: 23670899. https://doi.org/10.2967/jnumed.112.115964

8. Im HJ, Kim TS, Park SY, Min HS, Kim JH, Kang HG et al (2012) Prediction of tumour necrosis fractions using metabolic and volumetric 18F-FDG PET/CT indices, after one course and at the completion of neoadjuvant chemotherapy, in children and young adults with osteosarcoma. Eur J Nucl Med Mol Imaging 39(1):39–49. https://doi.org/10.1007/s00259-011-1936-4 Epub 2011/09/29. PMID: 21953008

9. Thoeny HC, Ross BD (2010) Predicting and monitoring cancer treatment response with diffusion-weighted MRI. J Magnet Reson Imaging 32(1):2–16. https://doi.org/10.1002/jmri.22167

10. Lee SY, Jee WH, Jung JY, Park MY, Kim SK, Jung CK et al (2016) Differentiation of malignant from benign soft tissue tumours: use of additive qualitative and quantitative diffusion-weighted MR imaging to standard MR imaging at 3.0 T. Eur Radiol 26(3):743–754. https://doi.org/10.1007/s00330-015-3878-x Epub 2015/06/18. PMID: 26080796

11. Wang CS, Du LJ, Si MJ, Yin QH, Chen L, Shu M, Yuan F, Fei XC, Ding XY (2013) Noninvasive assessment of response to neoadjuvant chemotherapy in osteosarcoma of long bones with diffusion-weighted imaging: an initial in vivo study. PLoS One 8(8):e72679. https://doi.org/10.1371/journal.pone.0072679

12. Reichardt W, Juettner E, Uhl M, Elverfeldt DV, Kontny U (2009) Diffusion-weighted imaging as predictor of therapy response in an animal model of Ewing sarcoma. Invest Radiol 44(5):298–303. https://doi.org/10.1097/RLI.0b013e31819dcc84

13. Oka K, Yakushiji T, Sato H, Hirai T, Yamashita Y, Mizuta H (2010) The value of diffusion-weighted imaging for monitoring the chemotherapeutic response of osteosarcoma: a comparison between average apparent diffusion coefficient and minimum apparent diffusion coefficient. Skeletal Radiol 39(2):141–146. https://doi.org/10.1007/s00256-009-0830-7

14. Tirman PF, Bredella MA (2010) Diagnostic imaging: orthopedics (Vol. 1) Amirsys Incorporated. 0721629202, 9780721629209

15. Ottaviani G, Jaffe N. The epidemiology of osteosarcoma. Cancer Treat Res. 2009;152:3–13. https://doi.org/10.1007/978-1-4419-0284-9_1. PMID: 20213383.

16. Greenspan, Adam (2015) Orthopedic imaging: a practical approach, 6th edn. Lippincott Williams & Wilkins ISBN-13: 9781451191301

17. Yakushiji T, Oka K, Sato H, Yorimitsu S, Fujimoto T, Yamashita Y, Mizuta H (2009) Characterization of chondroblastic osteosarcoma: gadolinium-enhanced versus diffusion-weighted MR imaging. J Magnetic Res Imaging 29(4):895–900. https://doi.org/10.1002/jmri.21703

18. Bajpai J, Gamnagatti S, Kumar R, Sreenivas V, Sharma MC, Khan SA, Rastogi S, Malhotra A, Safaya R, Bakhshi S (2011) Role of MRI in osteosarcoma for evaluation and prediction of chemotherapy response: correlation with histological necrosis. Pediatr Radiol 41(4):441–450. https://doi.org/10.1007/s00247-010-1876-3

19. Messina C, Bignone R, Bruno A, Bruno A, Bruno F, Calandri M, Caruso D, Coppolino P, Robertis R, Gentili F, Grazzini I, Natella R, Scalise P, Barile A, Grassi R, Albano D (2020) Diffusion-weighted imaging in oncology: an update. Cancers 12(6):1493. https://doi.org/10.3390/cancers12061493

Publisher's Note